Steel and Composite Structures, *Vol. 27, No. 2 (2018) 185-192*
DOI: https://doi.org/10.12989/scs.2018.27.2.185

Experimental study on creep behavior of fly ash concrete filled steel tube circular arches

Wu T. Yan [1a], Bing Han [*1,2], Jin Q. Zhang [3b], Hui B. Xie [1c], Li Zhu [1d] and Zhong J. Xue [4e]

[1] *School of Civil Engineering, Beijing Jiaotong University, Shangyuancun 3, Haidian District, Beijing 100044, P.R. China*
[2] *Key Laboratory of Safety and Risk Management on Transport Infrastructures, Ministry of Transport, PRC, Beijing 100044, P.R. China*
[3] *Research Institute of Highway Ministry of Transportation, West Tucheng Road 8, Haidian District, Beijing 100088, P.R. China*
[4] *Beijing Road Engineering Quality Supervision Station, Panjiamiao 222, Fengtai District, Beijing 100076, P.R. China*

(*Received October 1, 2017, Revised January 13, 2018, Accepted February 25, 2018*)

Abstract. Fly ash can significantly improve concrete workability and performance, and recycling fly ash in concrete can contribute to a cleaner environment. Since fly ash influences pozzolanic reactions in concrete, mechanical behaviors of concrete containing fly ash differ from traditional concrete. Creep behaviors of fly ash concrete filled steel tube arch were experimentally investigated for 10% and 30% fly ash replacement. The axes of two arches are designed as circular arc with 2.1 m computed span, 0.24 m arch rise, and their cross-sections are all in circular section. Time dependent deflection and strain of loading and mid-span steel tube were measured, and long term deflection of the model arch with 10% fly ash replacement was significantly larger than with 30% replacement. Considering the steel tube strain, compressive zone height, cross section curvature, and internal force borne by the steel tube, the compressive zone height and structural internal forces increased gradually over time due to concrete creep. Increased fly ash content resulted in more significant neutral axis shift. Mechanisms for internal force effects on neutral axis height were analyzed and verified experimentally.

Keywords: creep; fly ash; concrete filled steel tubes; arch; experiment

1. Introduction

Combining the advantages of steel and concrete, concrete filled steel tube (CFST) construction has attracted attention for structural and bridge engineering during the last few decades (Duarte *et al*. 2018, Ouyang *et al*. 2017, Ren *et al*. 2014, Yang *et al*. 2015). The steel tube serve as a form to casting the concrete, reducing cost and improving construction efficiency, and the concrete filling enormously improves compressive element stability. The most important CFST merits are excellent compressive resistance, ductility, and energy dissipation due to the confinement provided by the steel tube (Patel *et al*. 2016, Zhang *et al*. 2007). Hence, CFST has been successfully applied for construction of long span arch bridges, which are mainly subjected to axial compressive force, including more than 300 long span CFST arches constructed in China during the past 30 years (Zhang *et al*. 2007), with the No. 1 Hejiang Bridge completed in 2012 having record 530 m span.

However, concrete creep may have negative influence on long term CFST behavior (Liu *et al*. 2015, Wang *et al*. 2011, Wu *et al*. 2016, Uy 2001). Creep can increase structural deflection. For example, consider the Yajisha Bridge in Guangzhou, China, a CFST arch bridge with 360 m span. Creep deflection of this bridge reached approximately 12 cm 1 year after opening to traffic (Xin and Xu 2003). More importantly, creep leads to significant stress redistribution between the steel tube and concrete, increasing the steel tube stress with time. In serious cases, this stress redistribution may significantly reduce CFST resistance capacity. Many previous studies have considered CFST creep deflection (Geng *et al*. 2014, Shrestha *et al*. 2011, Wang *et al*. 2007, Yang *et al*. 2015), thermal influences on CFST creep (Wang *et al*. 2013), CFST creep reliability (Ma and Wang 2015), structural dynamic behavior influences on creep (Ma *et al*. 2016), creep buckling (Bradford *et al*. 2011, Luo *et al*. 2016, Pi *et al*. 2011), etc. However, to the best of our knowledge, studies of creep behaviors of fly ash concrete filled steel tube arch are rare.

In practice, it becomes more and more common to use admixtures, such as fly ash, slag and limestone, to replace partial cement for better performances of concrete. Among them, the fly ash is the most widely used due to its easy availability and low costs. Because the fly ash can significantly improves concrete's workability and pumping properties, hence it is used as main admixture added into the concrete filled the steel tube, for better construction quality. Meanwhile, fly ash can induce pozzolanic reactions in concrete; hence mechanical behavior of fly ash concrete can significantly differ from traditional concrete (Day

*Corresponding author, Professor,
E-mail: bhan@bjtu.edu.cn
[a] Ph.D. Student, E-mail: yanwutong@bjtu.edu.cn
[b] Professor, E-mail: jq.zhang@rioh.cn
[c] Ph.D., E-mail: hbxie@bjtu.edu.cn
[d] Ph.D., E-mail: zhuli@bjtu.edu.cn
[e] Senior Engineer, E-mail: xuezhongjun@126.com

ISSN: 1229-9367 (Print), 1598-6233 (Online)

1990), such as, creep. According to the existing researches, low volume fly ash concrete (< 40% fly ash against total cementitious materials) has been shown to decrease creep with increasing fly ash content (Zhao *et al*. 2006).

The current study investigated fly ash concrete filled steel tube arch creep behavior experimentally for 10% and 30% fly ash replacement ratio. The findings will help identify long term CFST arch behavior the effects of fly ash replacement ratios.

2. Experiment procedure

2.1 Materials and mix proportions

The materials used for the experiment were as follows.

- Normal Portland cement (volume mean diameter is 22.97 μm).
- Class I fly ash conforming to GB 1596-91 (mean particle size is 5.38 μm).
- River sand (fineness modulus 2.7).
- Natural crushed stone aggregate (particle sizes ranging from 10 to 20 mm).
- Super plasticizer.
- Water.

Two series of concrete mixtures with a water-to-binder ratio 0.4 were fabricated with 10% and 30% replacement of total cementitious materials by fly ash. Table 1 shows mix proportions, and Table 2 shows chemical components of the cement and fly ash.

Table 1 Concrete mix proportions

Content	Mix 1	Mix 2
Cement (kg/m^3)	378	294
Fly ash (kg/m^3)	42	126
Water (kg/m^3)	162.5	162.5
Sand (kg/m^3)	809	809
Coarse aggregate (kg/m^3)	1029	1029
Super plasticizer (kg/m^3)	5.76	5.76
Fly ash substitution (%)	10	30

Table 2 Cement and fly ash chemical components

Chemical component	Fly ash (%)	Cement (%)
CaO	4.35	63.66
SiO_2	56.62	22.42
Al_2O_3	25.62	6.11
Fe_2O_3	5.42	4.34
MgO	1.27	0.92
Na_2O	0.45	0.22
K_2O	1.71	0.55
MnO	0.05	0.14
TiO_2	1.41	0.23
P_2O_5	0.73	0.05
SO_3	0.43	0.26
L.O.L	4.08	0.51

2.2 Concrete filled steel tube arches

Two CFST circular arches were constructed and tested for the two different concrete types, as shown in Table 3. The arch spans are all 2.5 m, and their computed spans are 2.1 m. The arch rise is 0.24 m, and the radius of circular arch axis is 2.4 m. The rise-to-span ratio of the arches is 1:8.75. Tube diameter and thickness were 114 and 2.5 mm respectively. The both ends of arches were fixed on the concrete pedestals, which were anchored to the floor by bolts. The steel tube was cold formed mild steel with specific yield strength 345 MPa, and concrete elastic modulus and cube compressive strength (150 mm × 150 mm × 150 mm) were tested at age of 28 d. Fig. 1 shows the experimental arrangement of the arches.

2.3 Loading scheme

A sustained load was applied on the test arches at 28 d concrete age. To ensure constant sustained load on the experimental arch members, a specific loading beam was designed according to the reaction frame principle (Fig. 2), which applied a reaction force using self-lock hydraulic

Fig. 1 Experimental arrangement of the arches

Table 3 Arch specimen design

Arch No.	Concrete types	Concrete elastic modulus at 28d (MPa)	Concrete cube compressive strength at 28d (MPa)	Steel elastic modulus (MPa)
GL-1	Mix 1	3.25×10^4	39.6	2.06×10^5
GL-2	Mix 2	3.22×10^4	38.4	2.06×10^5

Fig. 2 Loading arrangement

Fig. 3 Load distributing girder

jacks by stretching steel strands. This also helped to supplement load loss during later period. The applied load was equally divided into two ribs through a rigid beam (Fig. 3), and an incremental loading scheme, i.e., 20, 50, 70, and 90 kN, was used for the experiment, where each load was maintained for 2–3 minutes, and the deflection recorded. Once the maximum load step was reached (90 kN), the load was sustained until the creep test completed. During the creep test, the values of sustained loads were checked daily, and compensated for the load loss by self-lock hydraulic jacks according to measured data of force sensor.

2.4 Measurements

The displacements of specimens were measured by dial gauge at two loading sections as well as the mid-span section, and two other dial gauges were arranged at both fixed ends of the arches to monitor the horizontal displacement of the supports as shown in Fig. 4. Strain gauges were installed on the steel tube along the span direction, and the upper, lower, and central axis strains were all monitored in each installed section.

3. Results and analysis

3.1 Long term deflection

Fixed with concrete pedestal, the measured horizontal displacement of both ends of the arches is very small, even almost close to zero during the tests. The recorded maximum support horizontal displacement is 0.006 mm under initial loading, and keeps constant over time. Fig. 5 shows vertical deflection at the loading position over time, where the ordinate represents average deflection sections 1 and 3 (Fig. 4) of specimens with different fly ash replacement ratio. With the same loading condition, initial elastic deformations of GL-1 and GL-2 were 1.741 and 1.842 mm respectively, which indicates decreased concrete elastic modulus with increased fly ash content. Deflections increased rapidly over the first month, then the rate of change decreased gradually, and the curve approached constant approximately 60d after loading. GL-1 deflection was approximately 23% greater than GL-2 165d after loading, which illustrates less creep for increased fly ash content.

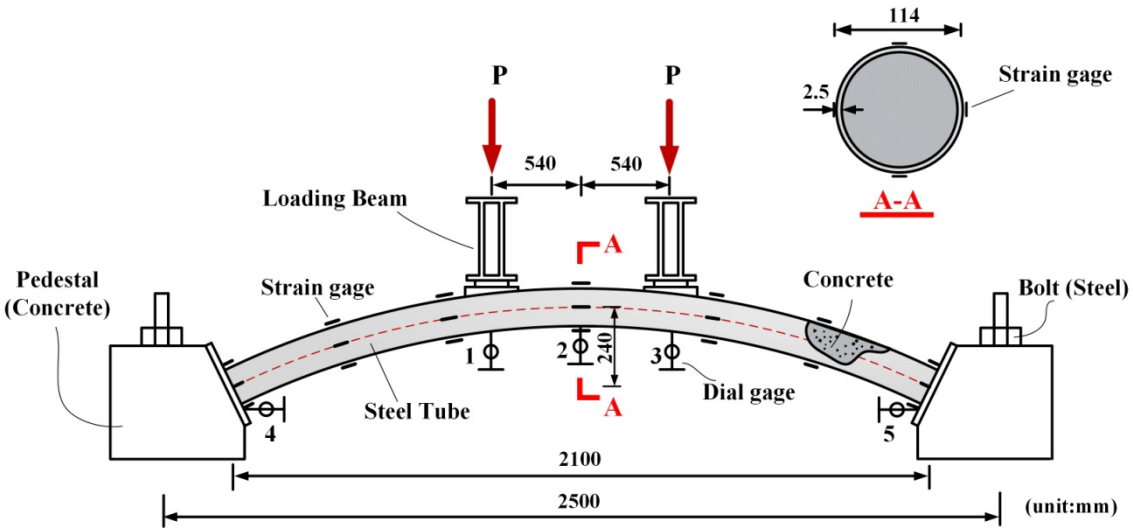

Fig. 4 Test setup and measurements

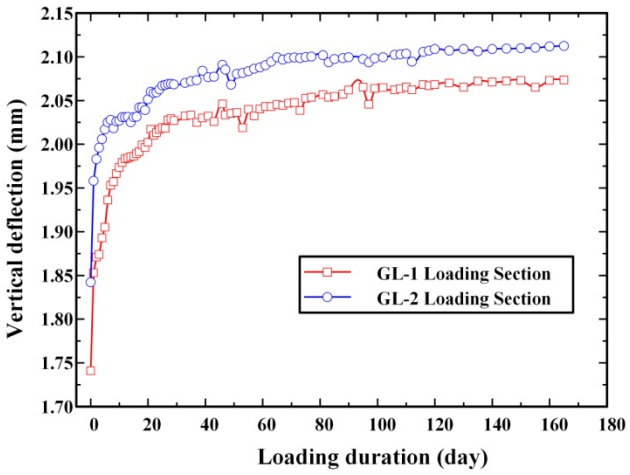

Fig. 5 Loading section deflection evolution

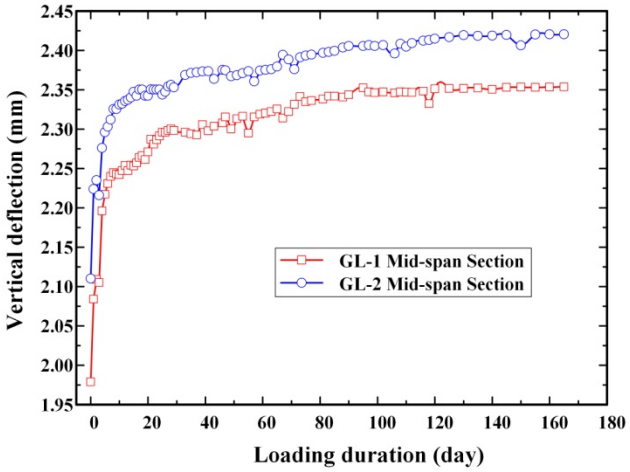

Fig. 6 Mid-span section deflection evolution

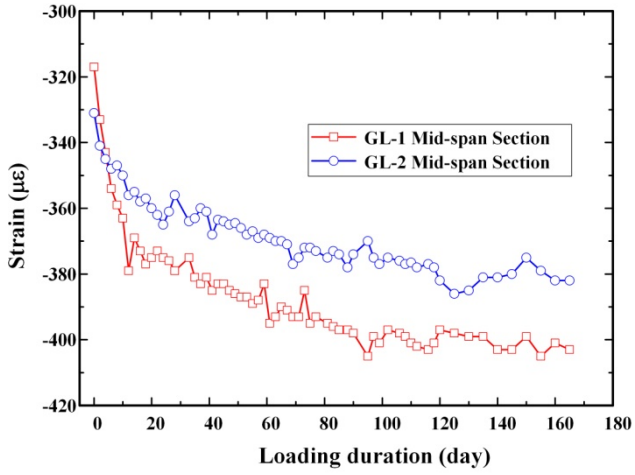

Fig. 7 Steel tube strain at mid-height of the mid-span section over time

Fig. 6 shows the deflection of mid-span section (Fig. 4) over time and the trends were similar to the ones of loading section (Fig. 5). GL-1 and GL-2 initial deflection at the mid-span section were 1.979 and 2.110 mm, respectively,

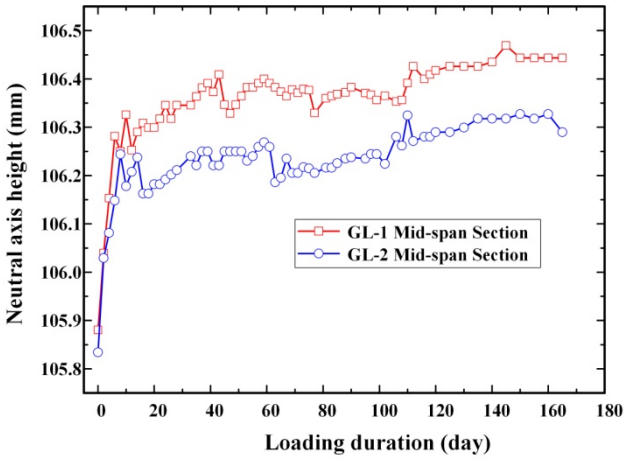

Fig. 8 Neutral axis height evolution

and deflection at 165d were 12.7% (GL-1) and 14.9% (GL-2) greater than those of the loading section. Long term deflection of GL-1 was approximately 20.60% greater than that of GL-2. Thus, fly ash content significantly influenced long term deflection in the section, which is consistent with the case in the loading section.

3.2 Steel tube strain

Fig. 7 shows steel tube strain at mid-height of the mid-span section (Section 2) over time, where the ordinate axis denotes average strain of both sides, and a negative value means compressive strain. The strain increases significantly with time, due to concrete creep. More significant stress increase occurred for GL-1, hence increased fly ash content reduced concrete creep.

Based on the plane section assumption, the neutral axis location can be deduced from the steel tube strain

$$h = \frac{\varepsilon_u H}{\varepsilon_u - \varepsilon_l} \tag{1}$$

where h denotes the neutral axis distance from upper edge of steel tube, u and l denote the strain of upper and lower portions of the steel tube, respectively, and H denotes the section height of the specimens.

Fig. 8 shows that the neutral axis height of the mid-span section shifts gradually downward with time, i.e., the height of the compressive zone increases.

The bending curvature of the section can be expressed as

$$\phi = \frac{\varepsilon_u - \varepsilon_l}{H} \tag{2}$$

where ϕ denotes the bending curvature of the cross section.

Fig. 9 shows that creep causes not only shift of neutral axis, as shown in Fig. 8, but also bending deformation of the arch. The neutral axis shift may be due owing to stress redistribution in the section, which is generally known as self-equilibrating internal stress. Since the arch is a statically indeterminate structure, creep can also cause secondary stress, which exhibits as the change of bending

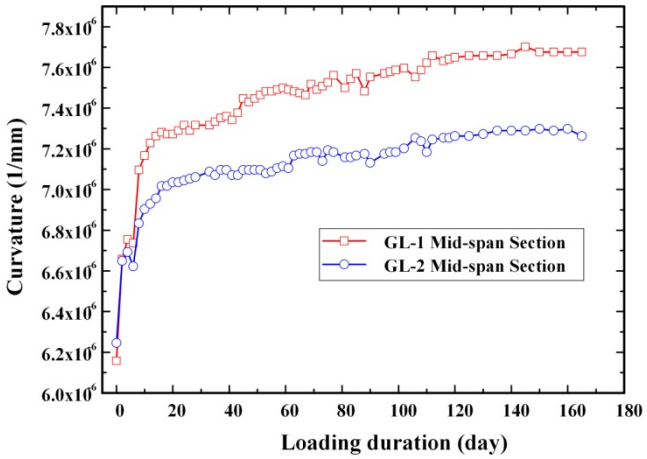

Fig. 9 Mid-span section curvature evolution

moment or curvature shown in Fig. 9. Stress redistribution is influenced by fly ash replacement ratio, with GL-1 curvature being significantly larger than GL-2.

3.3 Internal force over time

Internal force redistribution will occur in the structure due to concrete creep. It is reasonable to assume that the concrete elastic modulus remains constant during the test period for 28 d concrete loading age, by which time the development of concrete elastic modulus has been largely completed. Thus, assuming constant structural stiffness, redistribution and time-dependent variation of specimen internal force can be analyzed from steel tube strain changes over time.

With the prescribed loading conditions, the calculated axial force and bending moment of the mid-span cross sections were 136.5 kN and 3.26 kNm, respectively. The internal forces can be expressed as

$$N = (E_s A_s + E_c A_c)\varepsilon_m \tag{3}$$

and

$$M = (E_s I_s + E_c I_c)\phi \tag{4}$$

where N and M denote the measured axial force and bending moment of the section, calculated from the test strain data; E_s, A_s, and I_s denote the elastic modulus, area, and inertial moment of the steel tube; E_c, A_c, and I_c denote the elastic modulus, area, and inertial moment of the concrete; and ε_m and ϕ denote the measured central axis strain of steel tube and the sectional curvature.

Figs. 10 and 11 show axial force and bending moment in the mid-span section over time. Intial axial force and bending moment for GL-1 are 151.6 kN and 3.06 kNm, and for GL-2 they are 157.4 kN and 3.09 kN·m, respectively. Thus, GL-2 is a little larger than GL-1, which is consistent with the calculated results. Axial force and bending moment both tend to increase over time, which means that internal force transmission occured due to concrete creep.

The axial force increment for GL-1, with 10% fly ash replacement ratio, was 21.34% of the initial state at 165 d, and increment bending moment was 19.77%, whereas for GL-2 these are 13.35% and 14.01%, respectively. Thus, increasing of fly ash content decreased the redistribution of structural internal force.

4. Discussion

Previous studies of concrete creep have mainly focused on traditional concrete. However, with gradual awareness regarding environmental protection, fly ash industrial waste has become widely used in concrete engineering. The relatively few studies regarding creep of fly ash concrete have shown that the creep decreases with increasing fly ash content for fly ash ratios < 40% (Hill *et al*. 2003).

The current paper investigated creep behavior of fly ash CFST arches experimentally, and showed that creep deflection of specimens with high fly ash content was significantly less than specimens with low fly ash content.

For CFST structures, concrete creep increases steel tube stress and decreases core concrete stress. For the tested arches, mid-span section curvatures were deduced from the strain at the top and bottom fiber of the steel tubes, and we showed that mid-span section curvature increases with time. Hence, more stress is transferred to the bottom fiber of the

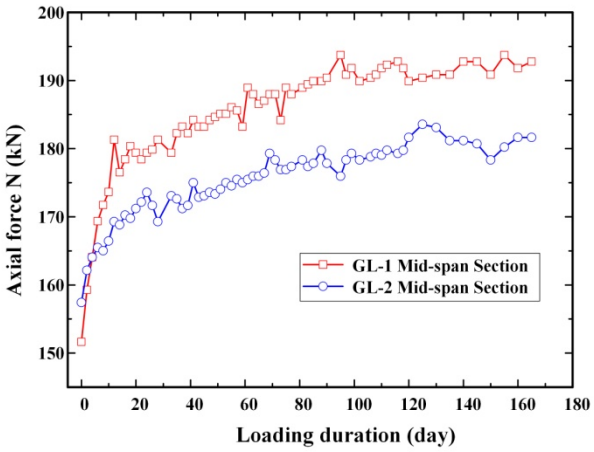

Fig. 10 Axial force in mid-span section evolution

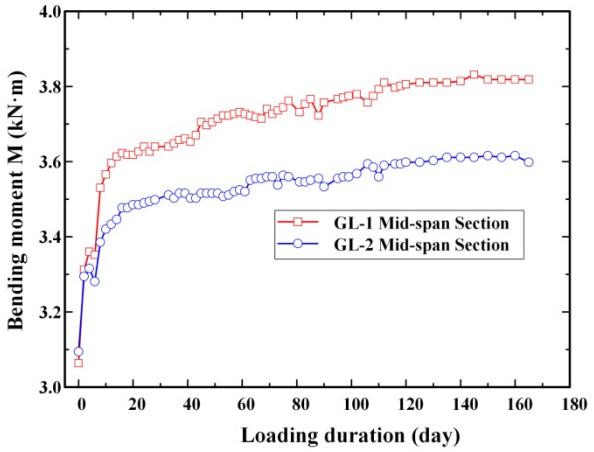

Fig. 11 Bending moment in mid-span section evolution

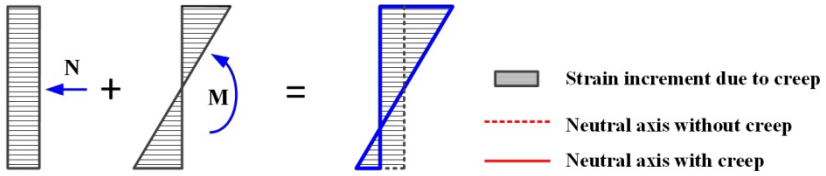

(a) Strain components of cross section

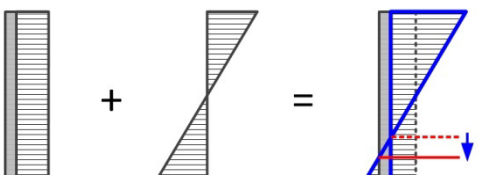

(b) Effects of axial creep on neutral axis

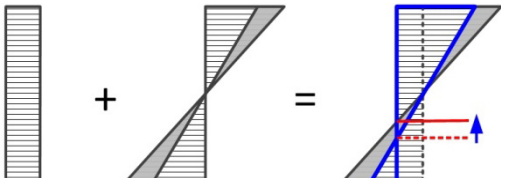

(c) Effects of bending creep on neutral axis

Fig. 12 Creep effects of axial force and moment on the neutral axis

steel tube. Therefore, the mechanism of increasing CSFT long term deflection includes not only axial shortening caused by creep, but also increased flexural curvature caused by stress redistribution between the steel tube and concrete. Figs. 10 and 11 showed that stress redistribution was more significant for relatively lower fly ash content, which directly caused larger curvature and deflection increments.

Elements subjected to combinations of axial force and bending moment would develop creep effects. With constant moment, axial force creep effects induce increasing axial deformation and the neutral axis shifts downward over time, as shown in Fig. 12(b). On the other hand, the neutral axis shifts upward over time due to increasing moment, as shown in Fig. 12(c). Thus, axial compressive strains of mid-height steel tube fibers (Fig. 9), which reflect axial creep caused by axial force, and mid-span section curvature (Fig. 11), due to bend creep, both increase with time. However, mid-span neutral axis heights tend to decrease (Fig. 10), because the high axial force and relatively low moment in the mid-span section under loading means that axial force creep effects on neutral axis heights are more significant.

The proposed mechanism of internal force affecting the neutral axis height may be verified from the test results. With constant axial force, the neutral axis height can be expressed as

$$h_M(t) = \frac{h}{2} - \frac{\varepsilon_{m,0}}{\phi_t} \tag{5}$$

where $\varepsilon_{m,0}$ denotes the measured steel tube strain of steel at mid-height of the section 0 d after loading, ϕ_t denotes measured time dependent curvature, and $h_M(t)$ denotes the neutral axis height to the upper edge of the cross section considering only effects of bending moment. Assuming constant bending moment, the neutral axis height due to axial force can be expressed as

$$h_N(t) = \frac{h}{2} - \frac{\varepsilon_{m,t}}{\phi_0} \tag{6}$$

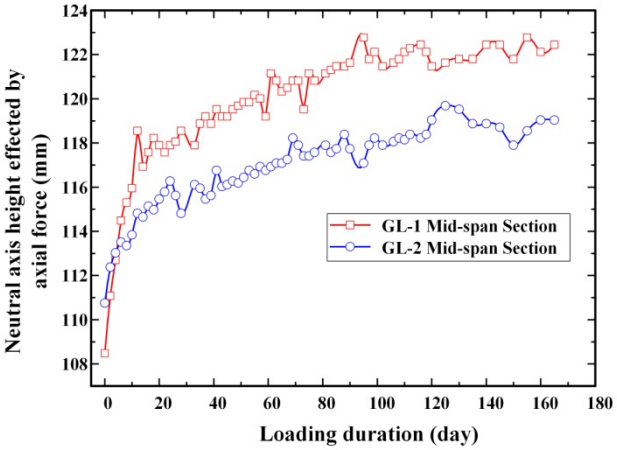

Fig. 13 Effects of axial creep on the neutral axis

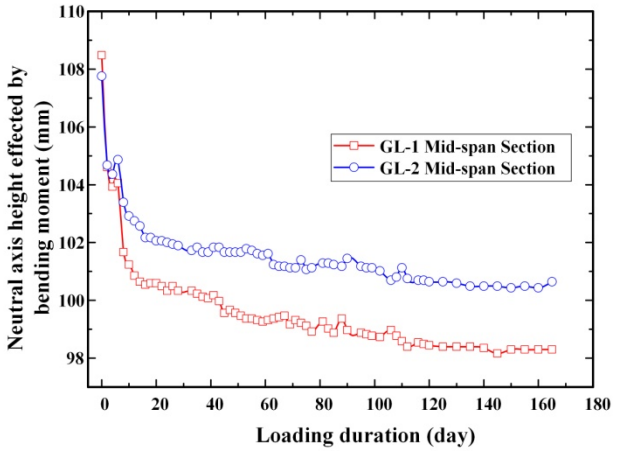

Fig. 14 Effects of bending creep on the neutral axis

where $\varepsilon_{m,t}$ denotes the measured steel tube strain at mid-height with development time t, ϕ_0 denotes the initial curvature at 0d after loading, and $h_N(t)$ denotes the neutral axis height to the upper edge of the cross section. Figs. 13 and 14 show the neutral axis height calculated from Eqs. (5)

and (6), respectively, are consistent with the proposed mechanism.

The downward shift of the neutral axis means more of the section region becomes compressive, and compressive strain on the steel tube upper section will increase over time. From the neutral axis location and section eccentricity, the specimen belongs to small eccentric compression member, which will eventually lead to crush failure under the limit load. Therefore, specimen bearing capacity will decrease with creep development, and hence fly ash plays a positive role in structural bearing capacity.

It should be pointed out that the CFST presents very complex behaviour under loading. There are many factors would take their effects on the creep, e.g., debonding between the concrete core and the steel tube, or splitting crack in the concrete core. In confined concrete under compression or bending, concrete will initiate tensile splitting crack at certain axial strain. After the onset of splitting cracks, the lateral-axial strains development will be more rapid and the confining stress will also change (Dong *et al*. 2015, Kwan *et al*. 2015). Naturally, the mechanical and creep behavior of the CFST structure will also be affected. In particular in CFST columns and arches, the delay in the onset of splitting cracks can be benefit of the structural performance. However, the cracking of the concrete core is difficult to be observed and not carried out in the experiment directly. If these factors could be considered, maybe the creep behavior of the CFST structures would be explained better.

5. Conclusions

Creep behavior of fly ash concrete filled steel tube arches and long term deflection and steel tube stress were investigated experimentally. Experimental and analysis outcomes confirm that creep influence on long term CFST behavior are significant. The main findings of this work are as following:

- Creep increases not only deflection of the arches, but more importantly, also bending curvature and neutral axis height of cross-section at the middle-span.
- The influence mechanism of axial force and bending moment on the neutral axis during creep is probed into and verified according to experimental results. The axial force increases neutral axis height, however the bending moment will have the opposite effect.
- It's also found in the experiment that deflection of the arch will decrease along with increase of fly ash content due to the creep.

Acknowledgments

The research described in this paper was financially supported by the China National Natural Science Foundation (grants 51608031, 51278037, and 51678030).

References

Bradford, M.A., Pi, Y.L. and Qu, W. (2011), "Time-dependent in-plane behaviour and buckling of concrete-filled steel tubular arches", *Eng. Struct.*, **33**(5), 1781-1795.

Day, R.L. (1990), "Strength, durability and creep of fly ash concrete Part II: Serviceability and durability of construction materials", *Proceedings of the First Materials Engineering Congress*, Denver, CO, USA, August.

Dong, C.X., Kwan, A.K.H. and Ho, J.C.M. (2015), "A constitutive model for predicting the lateral strain of confined concrete", *Eng. Struct.*, **91**, 155-166.

Duarte, A.P.C., Silvestre, N., de Brito, J., Júlio, E. and Silvestre, J.D. (2018), "On the sustainability of rubberized concrete filled square steel tubular columns", *J. Cleaner Prod.*, **170**, 510-521.

Geng, Y., Wang, Y.Y., Ranzi, G. and Wu, X.R. (2014), "Time-dependent analysis of long-span concrete filled steel tubular arch bridges", *J. Bridge Eng.*, **19**(4), 04013019.

Hill, R.L., Thomas, M.D.A., Obla, K.H. and Shashiprakash, S.G. (2003), "Properties of concrete containing ultra-fine fly ash", *ACI Mater. J.*, **100**(5), 426-433.

Kwan, A.K.H., Dong, C.X. and Ho, J.C.M. (2015), "Effects of confining stiffness and rupture strain on performance of FRP confined concrete", *Eng. Struct.*, **97**, 1-14.

Liu, H., Wang, Y.X., He, M.H., Shi, Y.J. and Waisman, H. (2015), "Strength and ductility performance of concrete-filled steel tubular columns after long-term service loading", *Eng. Struct.*,**100**, 308-325.

Luo, K., Pi, Y.L., Gao, W. and Mark, A.B. (2016), "Long-term structural analysis and stability assessment of three-pinned CFST arches accounting for geometric nonlinearity", *Steel Compos. Struct., Int. J.*, **20**(2), 379-397.

Ma, Y.S. and Wang, Y.F. (2015), "Creep influence on structural dynamic reliability", *Eng. Struct.*, **99**, 1-8.

Ma, Y.S., Wang, Y.F., Su, L. and Mei, S.Q. (2016), "Influence of creep on dynamic behavior of concrete filled steel tube arch bridges", *Steel Compos. Struct., Int. J.*, **21**(1), 109-122.

Ouyang, Y., Kwan, A.K.H., Lo, S.H. and Ho, J.C.M. (2017), "Finite element analysis of concrete-filled steel tube (CFST) columns with circular sections under eccentric load", *Eng. Struct.*, **148**, 387-398.

Patel, V.I., Uy, B., Prajwal, K.A. and Aslani, F. (2016), "Confined concrete model of circular, elliptical and octagonal CFST short columns", *Steel Compos. Struct., Int. J.*, **22**(3), 497-520.

Pi, Y.L., Bradford, M.A. and Qu, W. (2011), "Long-term non-linear behaviour and buckling of shallow concrete-filled steel tubular arches", *Int. J. Non-Linear Mech.*, **46**(9), 1155-1166.

Ren, Q.X., Hou, C., Lam, D. and Han, L.H. (2014), "Experiments on the bearing capacity of tapered concrete filled double skin steel tubular (CFDST) stub columns", *Steel Compos. Struct., Int. J.*, **17**(5), 667-686.

Shrestha, K.M., Chen, B.C. and Chen, Y.F. (2011), "State of the art of creep of concrete filled steel tubular arches", *KSCE J. Civil Eng.*, **15**(1), 145-151.

Uy, B. (2001) "Static long-term effects in short concrete-filled steel box columns under sustained loading", *ACI Struct. J.*, **98**(1), 96-104.

Wang, Y.F., Han, B., Du, J.S. and Liu, K.W. (2007), "Creep Analysis of Concrete Filled Steel Tube Arch Bridge", *J. Struct. Eng. Mech., Int. J.*, **27**(6), 1-12.

Wang, Y.Y., Geng, Y., Ranzi, G. and Zhang, S. (2011), "Time-dependent behaviour of expansive concrete-filled steel tubular columns", *J. Constr. Steel Res.*, **67**(3), 471-483.

Wang, Y.F., Ma, Y.S., Han, B. and Deng, S.Y. (2013), "Temperature effect on creep behavior of CFST arch bridges", *J. Bridge Eng.*, **18**(12), 1397-1405.

Wu, D., Gao, W., Feng, J. and Luo, K. (2016), "Structural

behaviour evolution of composite steel-concrete curved structure with uncertain creep and shrinkage effects", *Compos. Part B*, **86**, 261-272.

Xin, B. and Xu, S.Q. (2003), "Creep analysis of long-span concrete filled steel tubular arch bridges", *Railway Standard Design*, **44**(4), 31-33. [In Chinese]

Yang, Y.F. (2015), "Modelling of recycled aggregate concrete-filled steel tube (RACFST) beam-columns subjected to cyclic loading", *Steel Compos. Struct., Int. J.*, **18**(1), 213-233.

Yang, M.G., Cai, C.S. and Chen, Y. (2015), "Creep performance of concrete-filled steel tubular (CFST) columns and applications to a CFST arch bridge", *Steel Compos. Struct., Int. J.*, **19**(1), 111-129.

Zhang, S.M., Liu, C.Y. and Wang, Y.Y. (2007), "Mechanical behavior and failure modes of Han River North Bridge under ultimate loads", *Proceedings of 8th Pacific Structural Steel Conference-Steel Structures in Natural Hazards*, Wairakei, New Zealand, May.

Zhao, Q.X., Sun, W., Zheng, K.R., Chen, H.S., Qin, H.G. and Liu, J.Z. (2006), "Influence of fly ash properties on the creep character of high performance concrete and its mechanism", *J. Chinese Ceram. Soc.*, **34** (4), 446-451.

CC